J Appl Electrochem (2011) 41:107–114
DOI 10.1007/s10800-010-0218-3

Chromium electrodeposition from [BMIm][BF_4] ionic liquid

S. Survilienė · S. Eugénio · R. Vilar

Received: 27 November 2009 / Accepted: 5 September 2010 / Published online: 8 October 2010

Abstract The electrodeposition of black chromium coatings from ionic liquid 1-butyl-3-methylimidazolium tetrafluoroborate with chromium chloride, and the chemical composition of the deposits are discussed in this article. The UV–Vis spectra recorded for chromium(III) species in 1-butyl-3-methylimidazolium tetrafluoroborate suggest that along with the chromium(III) complexes containing three ligands, there are some amounts of chromium species containing four ligands in the bath employed. The cathodic process of chromium electrodeposition in the employed ionic liquid is complicated by the electrochemical reduction of water molecules, which is followed by chemical disintegration of tetrafluoroborate ions. The surface morphology of black chromium films deposited potentiostatically (–1.5 to −2.0 V) at 85 °C shows nodules and microcracks increasing in size with cathodic potential. Analysis of the X-ray photoelectron spectra recorded from surface to depth of the deposit has shown that the black oxide-rich chromium coating consists of chromium in both oxide and metallic states with small impurities of other elements (fluorine, boron, carbon and nitrogen) and the surface is covered with a thin layer of organic substances. The results of this study show that 1-butyl-3-methylimidazolium tetrafluoroborate may be considered as a promising substitute of toxic Cr(VI) baths for black chromium plating.

Keywords Ionic liquids · Chromium species · Cyclic voltammograms · Black chromium films

S. Survilienė (✉)
Institute of Chemistry, A.Goštauto 9, 01108 Vilnius, Lithuania
e-mail: sveta@ktl.mii.lt

S. Eugénio · R. Vilar
Department of Materials Engineering, Instituto Superior Técnico, Technical University of Lisbon, Av. Rovisco Pais, 1049-001 Lisbon, Portugal
e-mail: s.eugenio@ist.utl.pt

R. Vilar
e-mail: rui.vilar@ist.utl.pt

1 Introduction

Metal finishing processes using traditional aqueous electrolytes have many disadvantages; therefore, ionic liquids (ILs) are considered as an alternative to aqueous media for the electrodeposition of metals. The metal reduction process in ILs is distinct from that in aqueous solutions because of differences in viscosity, conductivity, potential window, double layer structure, and so on. The electrodeposition of chromium from Cr(III) aqueous solutions is accompanied by intensive hydrogen evolution resulting in a decrease in current efficiency of chromium. It is expected that, using the ionic liquid as a solvent, the current efficiency of Cr may be higher than that in the aqueous solution.

Imidazolium-based cations are preferred for metal electrodeposition because of their superior viscosity and conductivity, among which 1-butyl-3-methylimidazolium is the most preferred due to its high conductivity [1]. Ionic liquids with a high ionic conductivity and low viscosity are generally highly fluorinated with anions such as BF_4^- and PF_6^- and show a wide potential window [2]. In the search for suitable IL for electrodeposition of Cr, it is necessary to consider the reduction potential of chromium and the potential window of the IL. However, wide electrochemical windows of IL alone are not sufficient to make the electrodeposition of metal possible. For example, attempts to electrodeposit titanium metal from its halides in different

ILs have failed because of poor solubility of reduced titanium intermediates owing to which only an ultra-thin layer of titanium sub-halides was detected on the substrate surface [3]. The data published in [4] show that pyrrole is able to effectively act as a nucleating agent for the electroreduction of titanium species in IL. Currently much attention is given to the use of a polymeric nucleating agent to assist the electrodeposition of the metal from ILs. Analysis of published data has shown that to nucleate some metals and to form good deposits from ILs, a polymeric nucleating agent or a substrate coated with conducting polymer may be used [4–8]. Deposition of pure metals and alloys of over 35 metals has been achieved from ILs. The mechanism of Al electroreduction and the nature of electroactive species in the ILs/$AlCl_3$ system are discussed in [9]. According to the data published by Forsyth et al. [10], the film formation on the metal surfaces is not a simple chemical interaction between the components of the IL and substrate but may involve electrochemical processes. ILs and reactions at the electrochemical interface are discussed by MacFarlane et al. in [11], where are summarized the results obtained in the area of lithium and conducting polymer electrochemistry.

The majority of works on electrodeposition of metals have focused on imidazolium due to a wide potential window [12, 13]. The potential window decreases in the presence of water because water molecules will aggregate making hydrogen evolution easier at the electrode surface. However, hydration water does not behave like bulk water, suggesting that the water is strongly associated with the chloride anions or the metal center, therefore, the potential window is limited by reduction of Cr(III) rather than water [14]. Little is known about electrodeposition of Cr or its alloys from ILs [15–17]. The results published by Abbott et al. [15] on the electrodeposition of crack-free chromium from the IL formed between choline chloride and $CrCl_3{\cdot}6H_2O$ are extremely encouraging because they give confidence that the ILs are promising candidates for commercial application in chromium plating. It is known that [BMIm][BF_4] may be used to stabilize very small ($\leq$5 nm) metal nanoparticles [18] and for the formation of stable Cr and other metals nanoparticles from metal carbonyl precursors [19].

Taking into account the data published on both the electrochemical behavior of 1-butyl-3-methylimidazolium tetrafluoroborate [20] and electrodeposition of several metals from this IL, it is reasonable to study [BMIm][BF_4] as a solvent for chromium plating. The aim of this research was to define the state of Cr(III) species in IL formed between [BMIm][BF_4] and $CrCl_3{\cdot}6H_2O$ and to examine some properties (the morphology and composition) of chromium coatings deposited from the employed IL.

2 Experimental procedures

The preparation of the electrolyte and the electrochemical experiments were performed in a glove box under argon atmosphere. The employed solution was obtained dissolving the appropriate amount of $CrCl_3{\cdot}6H_2O$ (Merck) in [BMIm][BF_4] without further purification and stirring the mixture under vacuum at room temperature during 96 h. The IL used for the experiments is [BMIm][BF4] (Merck, for synthesis $\geq$98%) with the average water content of 500 ppm. This IL contains $\leq$0.1% of halides (according to the manufacturer specification).

Cyclic voltammograms were recorded with an Autolab potentiostat/galvanostat (The Netherlands) in a three-electrode electrochemical cell under potentiodynamic conditions with a potential scan rate of 50 mV s^{-1}. A Pt plate was used as a counter electrode and a Pt wire (2 mm in diameter) as the quasi-reference electrode (RE) to which all potentials are referred. A Pt disc, Cu plate, or an AISI 304 austenitic stainless steel plate was used as working electrode. Before experiments, the surface of the working electrodes was polished with a corundum suspension and de-greased, rinsed with acetone, and dried with hot air. The Cu and stainless steel working electrodes were further immersed in a 1:1 HNO_3:H_2O solution, rinsed with acetone, and dried with hot air. The employed electrolyte was maintained at constant temperature using a thermostatic bath.

The absorption spectra of $CrCl_3{\cdot}6H_2O$ in both the water and [BMIm][BF_4] were recorded in the wavelength range of 300–800 nm using a UV–Vis spectrophotometer. The absorption spectrum of the aqueous solution was recorded immediately after the preparation of the solution. The absorption spectra of $CrCl_3{\cdot}6H_2O$ in the IL were measured immediately after mixing and after drying under vacuum for 96 h.

Black chromium films, 1–2 μm thick were deposited by constant-voltage electrolysis on both stainless steel and copper substrates from the electrolyte containing 0.36 M $CrCl_3{\cdot}6H_2O$ in [BMIm][BF_4] at 85 °C.

The morphology of the films was characterised by scanning electron microscopy (SEM). SEM images were acquired in the central zone of the electrode in 2–3 locations to ensure that they represent the morphology of the film.

Elemental analysis of the coatings was carried out by X-ray photoelectron spectroscopy (XPS). The spectra were recorded with an ESCALAB MK-II spectrometer (VG Scientific, UK) using Mg K_α radiation. The spectrometer had a base pressure of 1.33×10^{-7} Pa in the analyzer chamber. For sputter etching, the argon gas pressure was maintained at 5×10^{-3} Pa in the preparation chamber. Under these conditions, the chromium phase can be etched

at a rate of $\sim$0.2 nm min^{-1}. The proportion of each element in at.% was calculated from the area of a single peak. The empirical sensitivity factors of the elements were taken from Briggs and Seach [21], and the spectra recorded were compared with the standard ones. The maximum accuracy of the method is 0.1 at.%. The XPS spectra were submitted to a Shirley-type background subtraction and fitted with mixed Gaussian–Lorentzian functions using a standard program. The chemical states were identified by comparison of the experimental photoelectron binding energies (BE) with values found in the literature [22, 23].

3 Results and discussion

To select the appropriate electrode potentials for electrolysis in [BMIm][BF_4], a cyclic voltammogram was recorded using a Pt disc electrode. Figure 1 shows the electrochemical window (dotted line) of the employed IL extending from +1.0 to –2.5 V, following which $[BMIm]^+$ may be reduced at the cathode with succeeding reactions of dimerization and de-alkylation [20]. According to the published data [16] where Pt wire was used as the quasi-reference electrode, the electrochemical window of [BMIm][BF_4] is about 4.3 V (+1.8 to –2.5 V). The full line in Fig. 1 reflects the chromium deposition—dissolution processes occurring during cyclic polarization of a AISI 304 austenitic stainless steel electrode in the IL [BMIm][BF_4] containing 0.36 M $CrCl_3{\cdot}6H_2O$. The cyclic voltammogram shows an anodic peak at about +0.3 V that may be related to the dissolution of the chromium film formed from the beginning of polarization (at −2.0 V). After reversal at +2.0 V (sweeping negatively), the cathodic current rises sharply at approximately –1.0 V and

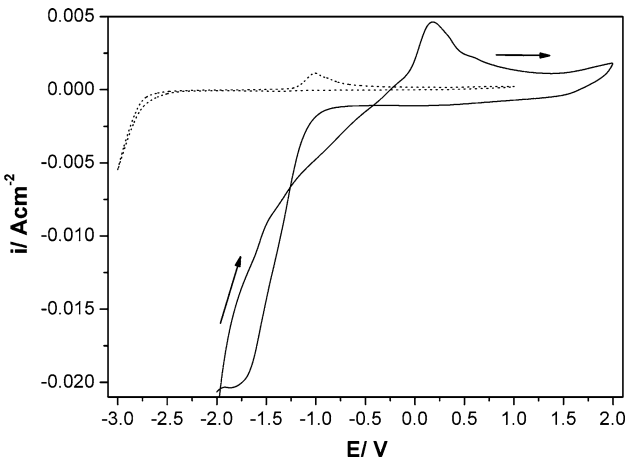

Fig. 1 Cyclic voltammograms recorded in [BMIm][BF_4] for a Pt disc electrode (*dotted line*) and in [BMIm][BF_4] + 0.36 M $CrCl_3{\cdot}6H_2O$ for an AISI 304 stainless steel substrate (*full line*) at 85 °C. Scan rate: 50 mV/s

reaches its limiting value at about –1.7 V, similar to what happens in an aqueous $CrCl_3$ electrolyte [24].

To identify the Cr(III) species in the $CrCl_3{\cdot}6H_2O$–[BMIm][BF_4] system, UV–Vis absorption spectra were recorded for $CrCl_3{\cdot}6H_2O$ in both the aqueous and employed IL solutions (Fig. 2). The spectra obtained in both cases show two absorption bands: a low wavelength band at about 430 nm in the aqueous solution (dashed line) and at 500 nm (dotted and full lines) in IL and a high wavelength at 630 and 700 nm, respectively. These spectra were compared with the positions of the absorption maxima of Cr(III) complexes in acid media published in [25], which are presented in Table 1. The data on the predominant species in $CrCl_3{\cdot}6H_2O$/choline chloride IL [26] were taken into account as well.

The data in Table 1 show that the number of chloride and water ligands in the Cr^{3+} complexes affect the UV–Vis spectrum of the solution. The substitution of each water molecule by a chloride ion, in the first coordination sphere, results in a shift of the lower wavelength band maximum by about 20–25 nm and the second band by 30–35 nm. The position of the low wavelength band in the aqueous

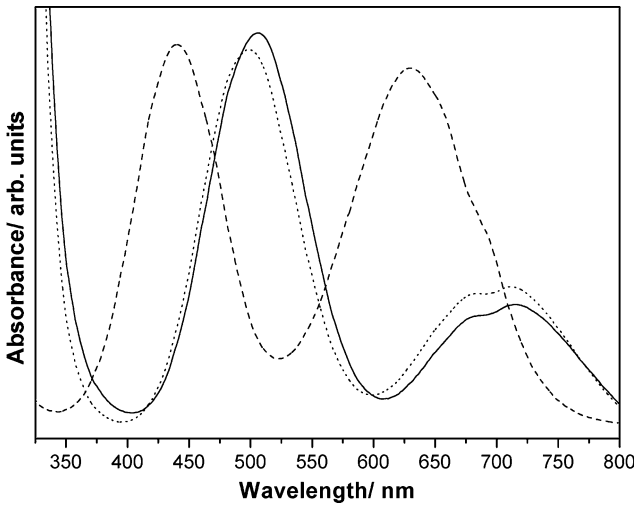

Fig. 2 Absorption UV-vis spectra of: 0.07 M $CrCl_3{\cdot}6H_2O$ aqueous solution (*dashed line*) and 0.02 M $CrCl_3{\cdot}6H_2O$–[BMIm][BF_4] IL recorded immediately after dissolution (*dotted line*) and after drying under vacuum for 96 h (*full line*)

Table 1 The literature data [25] on the positions of the absorption maximum (nm) of Cr(III) complexes obtained in acid media

Cr complex	Absorption maximum (nm)	
	I	II
$[Cr(H_2O)_6]^{3+}$	407	575
$[Cr(H_2O)_5Cl]^{2+}$	430	605
$[Cr(H_2O)_4Cl_2]^{+}$	450	635
$[Cr(H_2O)_3Cl_3]$	475	665

solution spectrum (dashed line in Fig. 2) agrees with the value for $[Cr(H_2O)_5Cl]^{2+}$ (Table 1), whereas the position of the high wavelength band points to the $[Cr(H_2O)_4Cl_2]^{+}$ complex. It is known, that the both $[Cr(H_2O)_5Cl]^{2+}$ and $[Cr(H_2O)_4Cl_2]^{+}$ species may dominate in a neutral aqueous environment, whereas the three-chlorine complex may be formed by the complete elimination of solvent water in a non-aqueous medium [25]. According to the published data [15], the main chromium complex in the IL is $[Cr(H_2O)_3Cl_3]$, whereas, a pronounced shoulder detected at 700 nm in the UV–Vis spectrum is regarded by the authors as evidence for the presence of $[Cr(H_2O)_2Cl_4]^{-1}$ species [26]. Taking into account the data given above and the positions of the low and high wavelength bands in the spectra recorded for the employed IL which are shifted to the higher wavelengths by 25 and 30 nm, respectively, in comparison with those for $[Cr(H_2O)_3Cl_3]$ complex, it is not improbable that there are modifications in the coordination sphere around the chromium ion as a result of which a new chromium species with four ligands is formed. Therefore, it is believed that along with the $[Cr(H_2O)_3Cl_3]$ complex there are some amounts of chromium species containing four ligands in the bath employed. However, it is hardly possible to draw the true structure of this species from the data obtained. Some deviations in the positions of bands in the spectra recorded immediately (dotted line) and after the vacuum drying during 96 h (full line) may be conditioned by the transformation of chromium complexes which can be completed only within 3–4 h [25].

The Cr coatings deposited from the employed IL at –1.5 to –2.0 V were found to be black in color and exhibited good adherence to the substrate. Figure 3 shows the influence of the potential applied on the morphology of the coatings obtained on steel substrates. The coating obtained at –1.5 V consists of densely packed globular particles. The coatings obtained at more negative potentials (−1.7 and –2.0 V) show a cracked structure with a network of microcracks and spherical or cauliflower-like nodules (Fig. 3b, c). The surface morphology of Cr coating deposited on the Cu substrate at –1.5 V (Fig. 4) also shows nodules and microcracks, which are clearly defined at a higher resolution (Fig. 4c). It should be pointed out that microcracked coatings are typical of aqueous Cr(III) electrolytes. The cross-sectional SEM morphology obtained for the thick Cr deposit (Fig. 5) confirms the cauliflower-like formations in the coating. As adjacent cauliflower-like features grow, they seem to be impinging on each other, creating a compact film.

To determine the elemental composition and the valence states of elements in the top layers of Cr coating, the XPS spectra were recorded and identified from references in the XPS database [23]. Analysis of the data obtained indicated the presence of Cr2p, O1s, C1s, N1s, B1s, and F1s peaks. The deconvoluted spectra of Cr2p3 recorded before sputtering of the top layer and after different sputtering times show the presence of three components in each of these levels (Fig. 6). The intensity of Cr2p3 peak recorded on the surface (Fig. 6a) is much lower than that recorded in depth

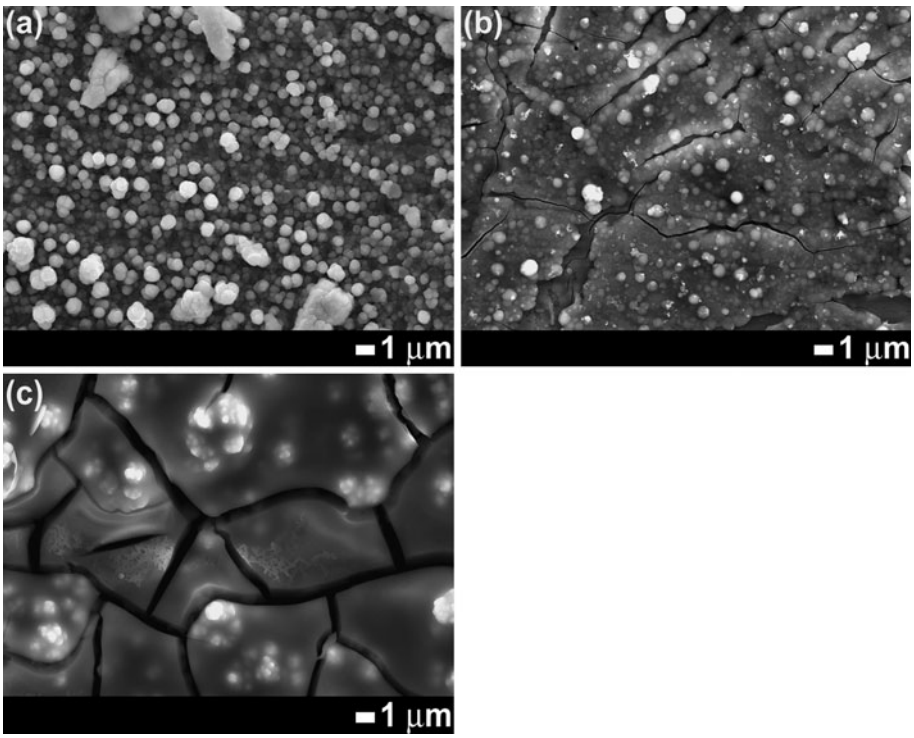

Fig. 3 SEM micrographs of black Cr coating deposited at 85 °C (1 h) on a steel substrate from the ionic liquid [BMIm][BF_4] + 0.36 M $CrCl_3 \cdot 6H_2O$ at: **a** −1.5 V. **b** −1.7 V. **c** −2.0 V: **a**, **b**, **c** ×5000

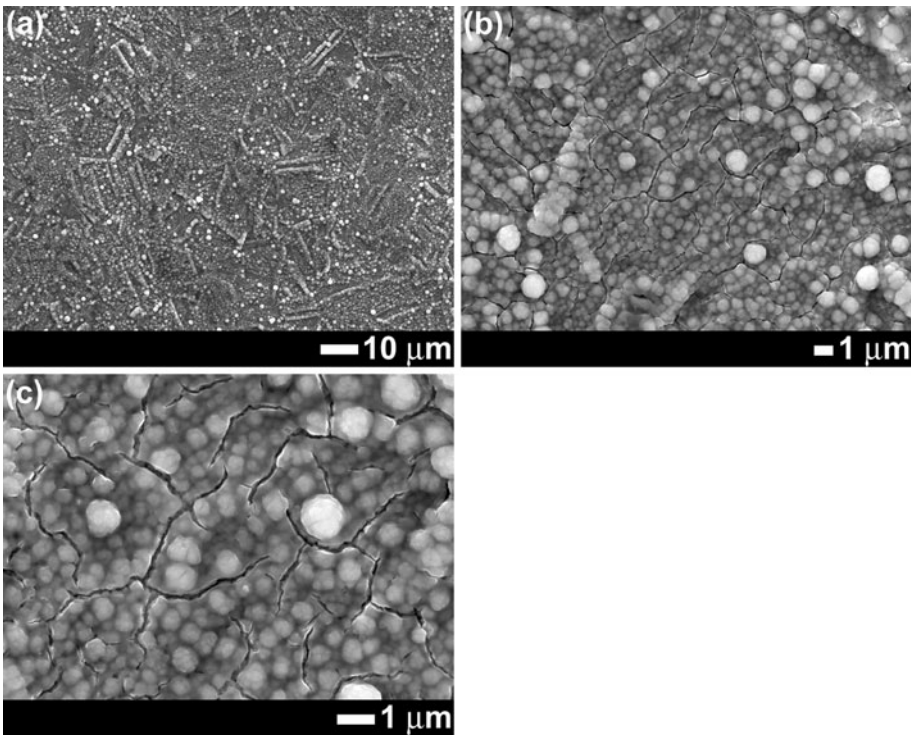

Fig. 4 SEM micrographs of black Cr coating deposited on the Cu substrate at 85 °C (15 min.) from the ionic liquid [BMIm][BF_4] + 0.36 M $CrCl_3 \cdot 6H_2O$ at −1.5 V: **a** ×1000 **b** ×5000 and **c** ×10000

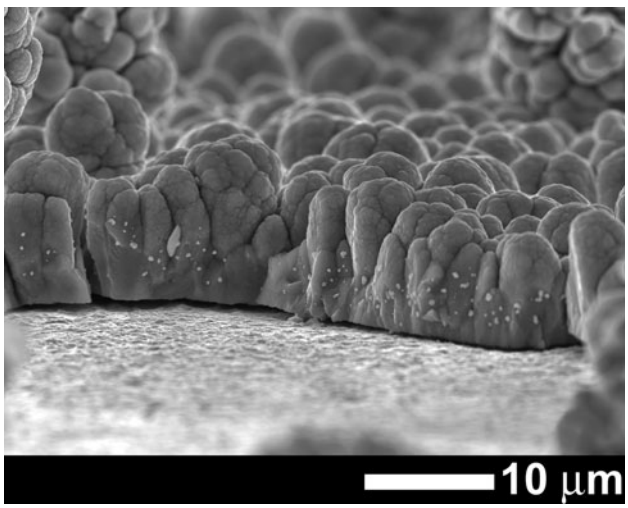

Fig. 5 A cross-sectional microstructure of black Cr deposited on the Cu substrate at 85 °C (2 h) from the ionic liquid [BMIm][BF_4] + 0.36 M $CrCl_3 \cdot 6H_2O$ at −1.5 V

of the deposit, which suggests the presence of adsorptive layer with the thickness ≤8 nm. For comparison, the coatings deposited from aqueous electrolytes are covered with a thick (about 20 nm) passive film consisting of chromium oxides and impurities of organic substances [27–29]. Although the positions of Cr2p3 peak corresponding to the metallic (BE = 574.5–575.2 eV) and oxide (BE = 576.5–577.9 eV) forms of chromium differ considerably (about 3 eV), the Cr2p3 peak is barely sensitive to the interaction of organic substances with Cr atoms [30, 31]. In contrast, the C1s spectra are the most informative ones to determine the nature of organic substances which may be both adsorbed on the surface and in the bulk of the deposit.

The data in Table 2 show that the C1s peaks recorded from surface to depth of the deposit are deconvoluted into three components, which suggest the presence of distinct carbon bounds. The high-energy components may be assigned to C–H and C–C bonds (BE = 288–289 eV), and to C–N and C = N bonds (BE = 286–287 eV) in the organic compound. It may be concluded that the thin top layer of Cr coating (about 8 nm) is mainly composed of organic substances ($[BMIm]^+$). After argon sputtering, a low-energy component with BE = 282.8 ± 0.1 eV emerges in the deconvoluted C1-s peak. It should be pointed out that a low-energy component is also observed in the C1s spectra recorded for Cr coatings deposited from aqueous electrolytes [32, 33], where the overall percentage of carbon generally is much higher (about 22 at.%) than that in the coating obtained from the employed IL (about 4–5 at.%). It is known [34–37], that C1s peak revealed at BE < 285.0 eV points to the presence of coordination bonds between carbon chains and chromium atoms and the negative shift value depends on the electronic density on carbon. Analysis of the C1s spectra makes it possible to illuminate the nature of species formed on the metal-electrolyte interface. As it follows from the data presented in Table 2, organic substances, apparently $[BMIm]^+$, are adsorbed on the surface of cathode, and a small amount of

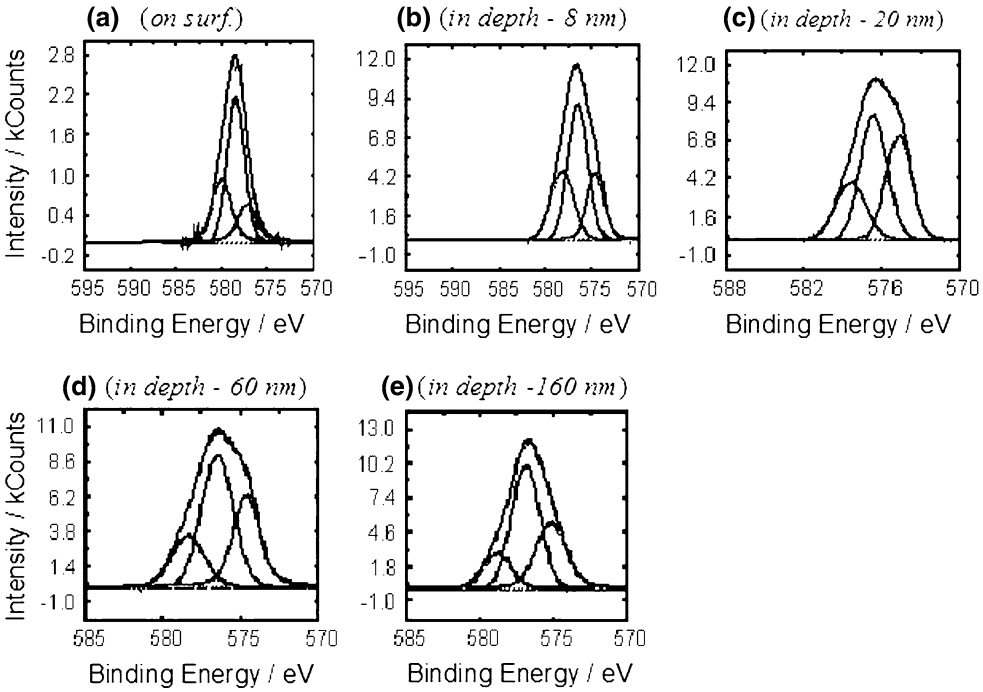

Fig. 6 XPS spectra Cr2p3 recorded before (**a**) and after argon sputtering (**b**, **c**, **d**, **e**) for the black Cr coating deposited at –1.5 V from the ionic liquid [BMIm][BF_4] + 0.36 M $CrCl_3{\cdot}6H_2O$ at 85 °C

Table 2 XPS data obtained for the deconvoluted C1s peaks recorded before and after argon sputtering

Depth (nm)	BE (eV)	C1s (at.%)	Carbon bonds
0	289.0; 287.5	11.0	C–H and C–C bonds
	285.9	44.5	C–N and C=N bonds
8	288.9	0.6	C–H and C–C bonds
	285.16	7.3	C–N and C=N bonds
	282.75	1.1	Coordination bonds between carbon chains and Cr atoms
20	287.43	0.4	C–H and C–C bonds
	285.02	4.0	C–N and C=N bonds
	282.8	0.7	Coordination bonds between carbon chains and Cr atoms
60	285.1	2.1	C–N and C=N bonds
	283.7; 282.9	2.5	Coordination bonds between carbon chains and Cr atoms
160	285.8	1.3	C–N and C=N bonds
	284.2; 282.7	3.3	Coordination bonds between carbon chains and Cr atoms

them may be captured by the increasing deposit during electrolysis. The values of binding energy determined from N1s peaks also may be attributed to the presence of $[BMIm]^+$ in both the surface and bulk of the deposit.

Figure 7 shows that the O1s peaks are deconvoluted in two main components, which may be attributed to Cr_2O_3 (BE = 530.6 ± 0.1 eV) and CrOOH (BE = 531.8 ± 0.2 eV). The presence of non-stoichiometric Cr oxides CrO_x (CrO, Cr_2O_3) in bulk of the deposit is also revealed from the highest intensity Cr2p3 peak (BE = 576.6 ± 0.2 eV). The data in Table 3 show that the metallic Cr (Cr2p3 peak at BE = 574 ± 0.1 eV) is detected only after sputtering of the top layer (8 nm) and its percentage increases in depth of the deposit. It follows from Table 3 that the percentage of oxygen is two-fold higher than that of Cr_{ox} (the total amount of chromium in oxide forms), and that the $[Cr_{ox}]/[O]$ ratio is kept constant through the depth of the deposit. This fact counts in favor of CrOOH (oxy-hydro-chromium). The positions of both the high-energy Cr2p3 peak (BE = 578.4 ± 0.2) and the F1s peaks point to the presence of CrF_2 [23] in the deposit. It should be mentioned that Forsyth et al. [10] studied the mechanism of metal fluorides formation on the metal substrate in ILs.

The data obtained can be explained taking into account the results of thermogravimetric analysis obtained by Abbot et al. [14, 15], according to which, at about 85 °C three water molecules are released and become uncoordinated to the Cr center. As such, water molecules behave similar to the bulk ones, the cathodic process occurring in the system studied may be presented through the following reactions:

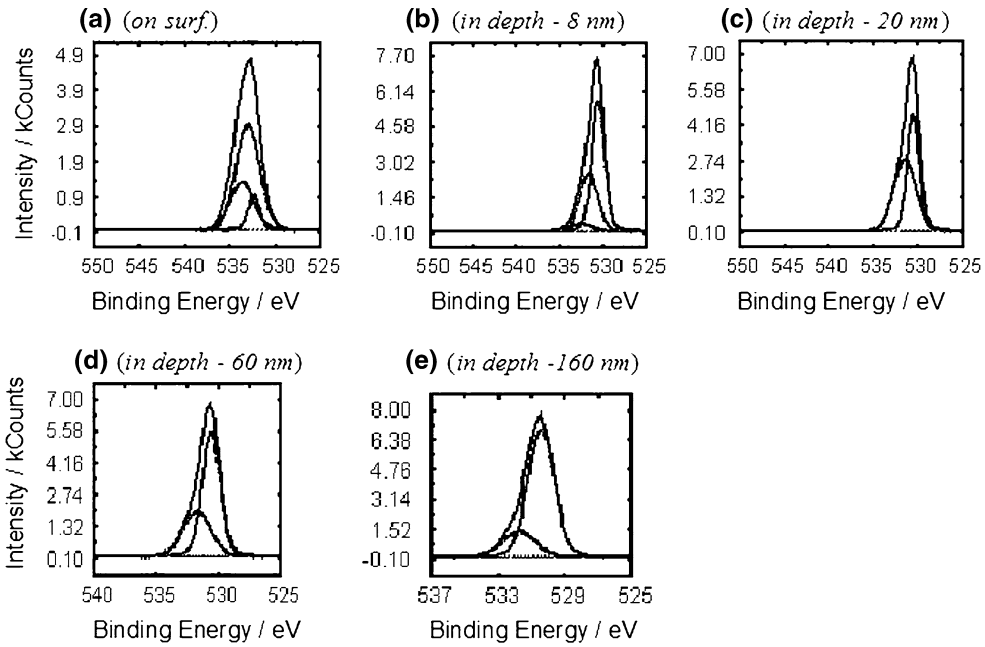

Fig. 7 XPS spectra O1s recorded before **a** and after argon sputtering (**b**, **c**, **d**, **e**) for the black Cr coating deposited at –1.5 V from the ionic liquid [BMIm][BF_4] + 0.36 M $CrCl_3{\cdot}6H_2O$ at 85 °C

Table 3 The distribution of elements in at.% from surface to balk of black Cr coating

Depth	Cr2p3		O1s		F1s		B1s at.%	N1s at.%	C1s at.%
	BE (eV)	at.%	BE (eV)	at.%	BE (eV)	at.%			
Top	577.3	1.0	532.4	3.5	685.4	2.6	0.9	2.47	55.42
	578.5; 580.0	4.3	533.0; 533.7	29.4					
8 nm	574.6	7.4	530.5	28.5	684.9	1.7	1.6	0.62	9.06
	576.5	16.9	531.6	17.2	685.1	3.8			
	578.2	9.9	532.6	2.9					
20 nm	574.6	7.7	530.7	36.6	685.0	6.1	1.1	0.9	5.1
	576.6	19.1	532	12.9					
	578.4	6.8							
60 nm	574.7	11.9	530.6	30.7	685.0	6.2	1.5	1.1	4.64
	576.6	18.5	531.7	16.7					
	578.5	7.5							
160 nm	574.7	11.9	530.5	41.7	684.9	4.1	1.6	1.3	4.62
	576.9	18.8	531.8	10.5					
	578.6	5.6							

$$Cr^{3+} + e \rightarrow Cr^{2+} \quad (1)$$

$$Cr^{2+} + 2e \rightarrow Cr^{0} \quad (2)$$

$$2H_2O + 2e \rightarrow H_2 + 2OH^-. \quad (3)$$

The emergence of OH^- ions leads to the formation of chromium hydroxide compounds. It is well known [38–40] that the electroreduction of Cr(III) complex ions proceeds in steps with the formation of intermediates—Cr(II) compounds. Accumulation of Cr(II) particles in the diffusion layer is responsible for the formation of Cr(II) compounds, such as CrF_2 and CrO, which are detected in the studied coatings. The formation of F^- ions at the near-cathode layer was possible owing to the emergence of OH^- ions which are responsible for the disintegration of BF_4^- [41]:

$$BF_4^- + 4OH^- \leftrightarrow B(OH)_4^- + 4F^-. \quad (4)$$

4 Conclusions

This article shows that 1-butyl-3-methylimidazolium tetrafluoroborate can be regarded as a promising bath material

to replace toxic Cr(VI) baths for black chromium plating. The following conclusions have been drawn from the present investigation:

- The UV–Vis spectra recorded for chromium(III) species in 1-butyl-3-methylimidazolium tetrafluoroborate suggest that along with the $[Cr(H_2O)_3Cl_3]$ complex, there are some amounts of chromium species containing four ligands in the bath employed.
- The surface morphology of the black Cr coatings deposited from the employed IL at –1.5 to −2.0 V shows nodules and microcracks increasing in size with the cathodic potential.
- Analysis of the XPS spectra recorded from surface to depth of the black Cr coating has shown that the deposit consists mainly of chromium in both oxide and metallic states with impurities of other elements (fluorine, boron, carbon, and nitrogen) and is covered with a thin layer (about 8 nm) of adsorbed organic substances.
- The data obtained suggest that during electrolysis, the water molecules, which were released from the inner coordination sphere of chromium(III) complex, reduced at the cathode giving OH^- ions which are responsible for the chemical disintegration of BF_4^- giving F^- ions to form CrF_2. Thus, the cathodic process of chromium electrodeposition is complicated by the electrochemical reduction of water molecules and chemical disintegration of the BF_4^- ions.

Acknowledgments Sónia Eugénio and Rui Vilar gratefully acknowledge the financial support from the European Community under the project IOLISURF (STRP-517002). Sónia Eugénio acknowledges with thanks a PhD grant from the Fundação para a Ciência e Tecnologia (FCT). The authors would like to thank Eng. Sílvia Quaresma for assistance in performing the UV–Vis spectrophotometry experiments, and V. Jasulaitiene, PhD. for the assistance during XPS experiments.

References

1. Tokuda H, Hayamizu K, Ishii K, Abu Bin Hasan Susan M, Watanabe M (2005) J Phys Chem B 109:6103
2. Fuller J, Carlin RT, Osteryoung RA (1997) J Electrochem Soc 144:3881
3. Endres F, El Abedin SZ, Saad AY, Moustafa EM, Borissenko N, Price WE, Wallace GG, MacFarlane DR, Newman PJ, Bund A (2008) Phys Chem Chem Phys 10:2189
4. Ding J, Wu J, MacFarlane D, Price WE, Wallace G (2008) Electrochem Commun 10:217
5. Ding J, Price WE, Ralph SF, Wallace GG (2004) Polym Int 53:681
6. Kang ET, Ting YP, Neoh KG, Tan KL (1995) Synth Met 69:477
7. Tsekouras G, Ralph SF, Price WE, Wallace GG (2004) Fobers Polym 5:1
8. Ding J, Misoska V, Price WE, Ralph SF, Tsekouras G, Wallace GG (2003) Synth Met 135–136:35
9. Rocher NM, Izgorodina EI, Rruther Th, Forsyth M, MacFarlane DR, Rodopoulos Th, Horne MD, Bond AM (2009) Chemistry: a Eur J 15:3435
10. Forsyth M, Neil WC, Howlett PC, Macfarlane DR, Hinton BRW, Rocher N, Kemp ThF, Smith ME (2009) ACS Appl Mater Interfaces 1:1045
11. MacFarlane DR, Pringle JM, Howlett PC, Forsyth M (2010) Phys Chem Chem Phys 12:1659
12. Noel MAM, Osteryoung RA (1996) J Electroanal Chem 293:139
13. Tierney BJ, Pitner WR, Mitchell JA, Hussey CL (1998) J Electrochem Soc 145:3110
14. Abbott Andrew P, McKenzie Katy J (2006) Phys Chem Chem Phys 8:4265
15. Abbott AP, Capper G, Davies DL, Rasheed R (2004) Eur J Clin Chem 10:3769
16. Bomparola R, Caporali S, Lavacchi A, Bardi U (2007) Surf Coat Technol 201:9485
17. Ali MR, Nishikata A, Tsuru T (1997) Electrochim Acta 42:2347
18. Vollmer C, Redel E, Abu-Shandi K, Thomann R, Manyar H, Hardacre C, Janiak C (2010) Chem Eur J 16:3849
19. Redel E, Thomann R, Janiak Ch (2008) *RSC ChemComm* 1789
20. Xiao Li, Johnson Keith E (2003) J Electrochem Soc 150(6):E307
21. D.Briggs, M.P.Seach, Analiz Poverkhnosti Metodami Ozhe I Rentgenovskoj Fotoelektronnoj Spectroskopii, Mir, Moskva, 1987
22. Wagner CD, Riggs WM, Davis LE, Moulder JF, Muilenberg GE, Handbook of X-ray Photoelectron Spectroscopy, Perkin-Elmer, Minneapolis, MN, 1978, p 190
23. Wagner CD, Naumkin AV, Kraut-Vass A, Allison JW, Powell CJ, Rumble JR Jr, NIST Standard Reference Database 20, Version 3.4 (Web Version)
24. Song YB, Chin D-T (2002) Electrochim Acta 48:349
25. Elving PJ, Zemel B (1957) J Am Chem Soc 79:1281
26. Abbott AP, Capper G, Davies DL, Rasheed RK, Archer J, John C (2004) Trans Inst Met Fin 82(1–2):14
27. Vykhodtseva LN, Edigaryan AA, Lubnin EN, Polukarov YuM, Safonov VA (2004) Russ J Electrochem 40:387
28. Lubnin EN, Edigaryan AA, Polukarov YuM (2000) Zashch Met 36:339
29. Vykhodseva LN, Kulakova II, Safonov VA (2008) Russ J Electrochem 44:877
30. Maurice V, Yang WP, Marcus P (1994) J Electrochem Soc 141:3016
31. Moffat TP, Latanision RM (1992) J Electrochem Soc 139:1869
32. Ramqvist L, Hamrin K, Johansson G, Fahlman A (1969) J Phys Chem Solids 30:1835
33. Survilienė S, Jasulaitienė V, Češunienė A, Lisowska-Oleksiak A (2008) J Solid State Ionics 179:222
34. Benziger JB, Madix RJ (1980) J Catal 65:36
35. Edigaryan AA, Safonov VA, Lubnin EN, Vykhodtseva LN, Chusova GE, Polukarov YuM (2002) Electrochim Acta 47:2775
36. Safonov VA, Vykhodtseva LN, Polukarov YuM, Safonova OV, Smolentsev G, Sikora M, Eeckhout SG, Glatzel P (2006) J Phys Chem B 110:23192
37. Vykhodtseva LN, Lubnin EN, Polukarov YuM, Safonov VA (2005) Russ J Electrochem 41:919
38. Danilov FI, Protsenko VS (2001) Zashch Met 37(3):251
39. Danilov FI, Protsenko VS, Butyrina TE (2001) Russ J Electrochem 37(7):826
40. Protsenko V, Danilov F (2009) Electrochim Acta 54:5666
41. Falicheva AI, Koroliova LD, Shalimov YuN (1971) Zashch Met 7(5):565